Cellular and Molecular Life Sciences (2022) 79:156
https://doi.org/10.1007/s00018-022-04130-7

ORIGINAL ARTICLE

Cell adhesion tunes inflammatory TPL2 kinase signal transduction

Maria Vougioukalaki[1,2] · Konstantina Georgila[3] · Emmanouil I. Athanasiadis[4] · Aristides G. Eliopoulos[2,3,4]

Received: 8 September 2021 / Revised: 22 December 2021 / Accepted: 3 January 2022 / Published online: 26 February 2022

Abstract

Signaling through adhesion-related molecules is important for cancer growth and metastasis and cancer cells are resistant to anoikis, a form of cell death ensued by cell detachment from the extracellular matrix. Herein, we report that detached carcinoma cells and immortalized fibroblasts display defects in TNF and CD40 ligand (CD40L)-induced MEK-ERK signaling. Cell detachment results in reduced basal levels of the MEK kinase TPL2, compromises TPL2 activation and sensitizes carcinoma cells to death-inducing receptor ligands, mimicking the synthetic lethal interactions between TPL2 inactivation and TNF or CD40L stimulation. Focal Adhesion Kinase (FAK), which is activated in focal adhesions and mediates anchorage-dependent survival signaling, was found to sustain steady state TPL2 protein levels and to be required for TNF-induced TPL2 signal transduction. We show that when FAK levels are reduced, as seen in certain types of malignancy or malignant cell populations, the formation of cIAP2:RIPK1 complexes increases, leading to reduced TPL2 expression levels by a dual mechanism: first, by the reduction in the levels of NF-κB1 which is required for TPL2 stability; second, by the engagement of an RelA NF-κB pathway that elevates interleukin-6 production, leading to activation of STAT3 and its transcriptional target SKP2 which functions as a TPL2 E3 ubiquitin ligase. These data underscore a new mode of regulation of TNF family signal transduction on the TPL2-MEK-ERK branch by adhesion-related molecules that may have important ramifications for cancer therapy.

Keywords TPL2 · ERK · Kinase · Adhesion · FAK · Apoptosis · SMAC mimetics

Introduction

Inflammatory signaling modulates cancer development and growth as well as responses to therapeutic interventions. Although much research has been devoted to dissecting individual cytokine-triggered signaling pathways, tumor progression and oncological outcomes are likely to be dictated by the interactions between inflammatory and other signals, including those triggered by growth factors and oncogenes. Delineation of the molecular events underlying such interactions will contribute to improved understanding of cell fate decisions and more options for targeting cancer growth and/or metastasis.

The tumor necrosis factor (TNF) superfamily has attracted significant attention for its diverse roles in the regulation of inflammation and immunity. Several TNF receptor (TNFR) family members have been found to also transduce competing signals that influence malignant cell survival *versus* death. Thus, stimulation of TNFR1 by TNF triggers a death pathway which is counteracted by the parallel activation of NF-κB and ERK signaling downstream of TNF Receptor Interacting Protein kinase 1 (RIPK1) [1]. These signals promote de novo synthesis of anti-apoptotic proteins or modify pre-existing regulators of apoptosis to maintain cell survival and enable the execution of the inflammatory program. Engagement of CD40, another TNFR family member, also triggers RIPK1-dependent carcinoma cell death which is manifested upon suppression of the survival arm of CD40 signaling entailing PI3K/AKT and ERK [2–4]. It could thus be envisaged that stimuli influencing

✉ Aristides G. Eliopoulos
eliopag@med.uoa.gr

1 Division of Basic Sciences, University of Crete Medical School, Heraklion, Greece

2 Institute for Molecular Biology and Biotechnology, Foundation of Research and Technology Hellas, Heraklion, Greece

3 Department of Biology, School of Medicine, National and Kapodistrian University of Athens, Athens, Greece

4 Center of Basic Research, Biomedical Research Foundation of the Academy of Athens, Athens, Greece

these pro-survival signaling pathways could impact cell fate decisions in response to TNFR1 or CD40 activation. Herein, we test the hypothesis that cell adhesion to extracellular matrix (ECM) provides a stimulus with a modifying effect on TNFR-activated pathways.

Cell adhesion to components of ECM is mediated by heterodimeric integrin receptors and impacts cell survival. Normal epithelial cells detached from ECM initiate a death program termed anoikis [5] to which cancer cells are resistant, a property that enables them to metastasize [6]. Focal Adhesion Kinase (FAK), a nonreceptor tyrosine kinase encoded by *PTK2*, conveys several adhesion-dependent survival signals, including binding to RIPK1 to prevent pro-death, caspase-containing complex formation [7]. Increased expression of FAK in certain malignancies and cancer cell lines is correlated with these actions and FAK has been proposed as a therapeutic target of high potential [8, 9]. In contrast, other studies have shown that reduced expression of FAK in the tumor stroma or the malignant cells is associated with amplified tumor growth [10, 11]. One hypothesis that could explain these seemingly contrasting observations is that FAK expression levels and activity can be dynamically regulated at the cross-road of inflammatory and survival pathways to confer different outcomes in a stimulus and cell type-dependent manner [11].

Our previous work in macrophages and B cells has shown that both TNFR1 and CD40-induced ERK signaling critically depend on the activation of the Tumor Progression Locus 2 (TPL2) kinase (also known as MAP3K8 and COT) [12, 13]. Mechanistically, the activity of TPL2 requires its dissociation from an inhibitory signaling complex containing p105 NF-κB1 and ABIN2 that is triggered by several stimulus-induced phosphorylation events. These are largely coordinated by the IκB kinase (IKK) complex which phosphorylates both p105 NF-κB1 leading to its proteolytic processing, and TPL2 at Thr^{290} and Ser^{400} that are required for TPL2 release from p105 [14] and kinase activity towards MEK, the ERK kinase [15–17]. IKK also phosphorylates IκBα, triggering its degradation and the release of IκBα-bound RelA (p65 NF-κB) which translocates to the nucleus and transactivates NF-κB target genes.

Besides being coupled to inflammatory signal transducers, TPL2 protein levels in malignant cells are also modulated by molecules with oncogenic potential, such as Skp2 (S-phase kinase-associated protein 2). Skp2 is an E3 ubiquitin ligase that is expressed at elevated levels in several tumors, serving as a prognostic marker and a promising therapeutic target [18, 19]. As part of the SCF^{Skp2} (Skp, Cullin, F-box containing complex) E3 ubiquitin ligase complex, it drives the degradation of various cyclin-dependent kinase inhibitors and tumor suppressors, such as such $p21^{Cip1}$, $p27^{Kip1}$, and $p57^{Kip2}$ and perturbs p53-dependent apoptosis [20]. Therefore, Skp2 has a prominent role in cell cycle, oncogenic transformation, epithelial mesenchymal transition, tumor progression and metastasis [18, 19]. A recent study placed Skp2 at the control of ubiquitin-mediated TPL2 turnover to facilitate $HER2^+$ breast cancer metastasis [20], supporting a link between TPL2 expression levels and cancer cell signaling. Indeed, the previous studies by us and others have shown that TPL2 expression is reduced in several types of malignancy and that endogenous TPL2 physiologically operates as a tumor suppressor in lung, skin and colon cancer [21–25]. Pertinent to the therapeutic exploitation of the reduced expression levels of TPL2 in human lung cancer [21] is the recently reported synthetic lethality of the combination of *TPL2* knockdown and TNF treatment in vitro [26].

In this study, we test the hypothesis that cell adhesion-emanating signals intersect TNFR family receptor pathways responsible for cell survival *versus* death. We reasoned that TPL2 may serve as a point of convergence of these interactions and show that carcinoma cells detached from ECM display defects in ERK activation in response to TNF or CD40 ligand (CD40L) at the level of TPL2. The data presented herein also identify a novel functional link between FAK and TPL2 which impacts TPL2 expression levels and activation status.

Materials and methods

Cell culture, reagents and treatments

EJ bladder carcinoma cells were maintained in RPMI medium supplemented with 10% FCS. HeLa cervical carcinoma cells, Human Embryonic Kidney 293 cells and Mouse Embryonic Fibroblasts were maintained in DMEM medium supplemented with 10% FCS. CD40-expressing fibroblasts and HeLa cells and recombinant soluble CD40L were described previously [27, 28]. *TPL2−/−* MEFs and HA-TPL2 expressing *TPL2−/−* MEFs were a kind gift of Prof. P. Tsichlis [14]. Recombinant human TNF and EGF were purchased from R&D Systems. TPL2 inhibitor (CAS 1186649-59-1) was purchased from Calbiochem (Sigma-Aldrich) and used at 20 μM to pre-treat cells for 1 h prior to stimulation and all along experimental treatments. For cell detachment assays, adhered cultures were treated with TrypLE Express (Gibco), kept in suspension with gentle agitation for 2–3 h and then plated on dishes covered with Fibronectin (F1141, Sigma-Aldrich) or Poly-L-Lysine (P8920, Sigma-Aldrich) and/or stimulated with appropriate ligands. Cells were allowed to adhere for 1 h to coated dishes before being treated with the ligands.

Antibodies

Antibody against phosphorylated ERK1/2 (M8159) was purchased from Sigma-Aldrich, β-actin (clone C4) from Millipore, anti-ERK1/2 (C-14), TPL2 (M20), α/β-tubulin (TU-02), GAPDH (0411), Sp1 (E-3), IκBα (L35A5), RIPK1 (C20) and FAK (D1) from Santa Cruz. Anti-MEK1/2$^{pSer217/pSer221}$, anti-p38$^{pThr180/pTyr182}$, anti-JNK$^{pThr183/pTyr185}$, anti-IKKα/β$^{pSer176/180}$, anti-p65 (#3034) and anti-STAT3^{pY705} were purchased from Cell Signaling Technologies. cIAP1/2 antibody (MAB3400) was purchased from R&D systems and anti-NFκB1 (AM06636SU-N) was from Acris/OriGene. IL-6 neutralizing antibody (MAB206) was purchased from R&D Systems and used at 10 ng/ml. We note that certain lots of anti-TPL2 (M20) Ab reacted with a nonspecific protein of approximately 62–64 kD (compare Figs. 5 and 3).

Cell death measurements

EJ bladder carcinoma cells attached to tissue culture dish or kept in suspension (for 3 h prior to stimulation) were either left untreated, treated with 0.5 μg/ml CD40L or treated with 100 ng/mL EGF prior to collection by centrifugation at 500 g for 5 min, and staining with SYTO^{TM}16/Propidium Iodide according to the instructions of the manufacturer (ThermoFisher). Assessment of cell death in HeLa cells was based on propidium iodide staining and nuclear morphology as previously described [3] and on a Cellular DNA Fragmentation ELISA that relatively quantifies the amount of histone-complexed DNA fragments during apoptosis (Roche, Cat. Number: 11585045001).

RNA interference

RNA interference was performed as previously described [3]. For FAK knockdown, the siGENOME SMARTpool Human PTK2 oligo mix containing 4 siRNAs (Dharmacon Life Technologies, MQ-003164–02) with the following target sequences: 5′-GCGAUUAUAUGUUAGAGAU-3′, 5′-GGGCAUCAUUCAGAAGAUA-3′, 5′-UAGUACAGCUCUUGCAUAU-3′ and 5′-GGACAUUAUUGGCCACUGU-3′; our blast search showed that these siRNAs align with human but not avian PTK2. The following siRNA oligos were used: TPL2 Silencer® Select siRNA, Ambion (ID: s3384 and s3385); for RIP1 knockdown the 5′-GUACUCCGCUUUCUGUAAA-3′ siRNA oligo was used, for cIAP1 and cIAP2 5′- UUCGUACAUUUCUCUCUUA-3′ and 5′-AAUGCAGAGUCAUCAAUUA-3′ siRNAs respectively, for CYLD knockdown, the 5′- GAAGGCUUGGAGAUAAUGA-3′ oligo and for TRAF2 knockdown siGENOME SMARTpool (M-005198; Dharmacon). As control, the siGENOME nontargeting siRNA pool#1 (D-001206-13-05; Dharmacon) or Luciferase (AM16204 Silencer® Select siRNA, Ambion) [3] was used as control. Transfection of cell lines was performed in two rounds using the RNAiMAX transfection reagent (Invitrogen), as previously described [3, 28]. For rescue experiments, MYC epitope-tagged (MT) chicken FAK (a gift from Dr V. Kostourou, Al. Fleming Institute, Athens, Greece) was co-transfected with HA epitope (HA)-ERK1 in HeLa cells using Lipofectamine 2000 (Invitrogen) according to the manufacturer's protocol following the 2nd round of siRNA transfection. Thirty-six hours later cells were stimulated with 50 ng/ml TNF (R&D systems, Catalog # 210-TA), lysed and processed for anti-HA immunoprecipitation and immunoblotting.

Preparation of protein extracts, immunobloting and immunoprecipitation assays

Following treatment, cells were washed with ice cold PBS and lysed in RIPA buffer (10 mM Tris–Cl (pH 8.0), 1 mM EDTA, 0.5 mM EGTA, 1% Triton X-1000, 1% sodium deoxycholate, 0.1% SDS, 140 mM NaCl) supplemented with protease and phosphatase inhibitors (complete™-ThermoFisher and PhosSTOP™- Merck, respectively) to isolate whole cell protein lysates. For preparation of nuclear extracts we followed the procedure we have previously described [27, 28]. Protein content was quantified using the Pierce™ BCA Protein Assay Kit (Thermo Scientific), according to the manufacturer's instructions and appropriate amount of cell lysate was loaded onto SDS-PAGE gels and transferred on nitrocellulose membranes using Tris–Glycine buffer (25 mM Tris, 192 mM Glycine, 20% (v/v) methanol, pH ~ 8.3). Protein probing was usually performed by incubation of nitrocellulose mebranes o/n with appropriate antibody dilutions in TBS/T buffer supplemented with 2% nonskimmed milk, following by washes in TBS/T and 1 h incubation with secondary antibody containing solution. Chemiluminescent signals were visualized with Pierce™ ECL Western Blotting Substrate (Thermo Fisher) either using films or iBright Imaging Systems (Thermo Fisher). Protein bands were quantified using the Image J Software.

For co-immunoprecipitation experiments of endogenous RIPK1 and cIAP1/2 proteins, HeLa cells were harvested following two rounds of transfection with FAK siRNA (one 10 cm 90% confluent dish per sample) in co-IP buffer (10 mM Tris–Cl (pH 8.0), 1 mM EDTA, 0.5 mM EGTA, 0,1% Triton X-1000, 50 mM NaCl, 5% glycerol) supplemented with protease and phosphatase inhibitors. Protein extracts were cleared from debris by centrifugation (13000 rpm, 10 min), quantified with Bradford assay so that equal amounts of total protein would be used in downstream procedures and 2 μg of anti-RIPK1 were added to each sample. Following overnight incubation at 4 °C with gentle agitation, 50μL of G-Sepharose beads (BD Biosciences),

were added for a further 2 h incubation period. The beads were washed at least 4 × with co-IP buffer and resuspended in equal volume of Protein Loading buffer. Samples were analysed with SDS-PAGE and immunobloting with the appropriate antibodies.

Immunoprecipitation of HA-ERK1 in rescue experiments was performed using the same methodology as above by applying mouse anti-HA antibody (12CA5, Roche) for pull-down of HA-ERK1, followed by immunoblotting using rabbit anti-phospho-ERK1/2 or goat anti-ERK1 antibodies.

Kinase assays

HA-TPL2-expressing MEFs were either kept attached on tissue culture plate or detached with TrypLE solution (Gibco) and kept in suspension for 2 h prior to cell lysis with lysis buffer [20 mM HEPES (pH 7.6), 250 mM NaCl, 0.5% NP-40, 20 mM β-glycerophosphate, 1 mM EDTA, 5 mg/ml p-nitrophenylphosphate (PNPP), 0.1 mM Na_3VO_4, 1 mM dithiothreitol (DTT), 1 mM phenylmethylsulfonyl fluoride (PMSF), and a protease inhibitor cocktail (Sigma-Aldrich)]. Lysates were cleared by centrifugation and immunoprecipitated with 2 μg of anti-HA (3F10, Merck) antibody for 2 h, followed by incubation with 25μL of G Sepharose beads for another 2 h. Beads were extensively washed with lysis buffer followed by 3 × washes with wash buffer (20 mM HEPES, pH 7.6, 20 mM $MgCl_2$, 20 mM β-glycerophosphate, 1 mM EDTA, and 2 mM DTT). Then, an equal volume of kinase reaction buffer [20 mM HEPES, pH 7.6, 20 mM $MgCl_2$, 20 mM β-glycerophosphate, 1 mM EDTA, and 2 mM DTT containing 20 μM ATP, 2 mM DTT] and 1 μg recombinant GST-MEK1 (14–420, Merck) was added and the samples were incubated at 37 °C with shaking for 30 min. Reactions were terminated with the addition of an equal volume of 2 × Protein Loading buffer and analyzed with western blot.

Luciferase assays

HeLa or A549 cells were transfected for one round with *PTK2* siRNA and control siRNA oligos and for a second round with both siRNA oligos and an NF-κB Luciferase (3Enh.kB-ConALuc containing three tandem repeats of the NF-κB sites from the Igk promoter, [29]) and Renilla Luciferase reporter plasmids. Cells were harvested 48 h after the second round of transfection, and Luciferase bioluminesce was measured with Promega's Dual-Luciferase reporter assay system, according to manufacturer's instructions.

RNA extraction, cDNA synthesis and qPCR

Total RNA was isolated using NucleoSpin RNA Kit (Macherey–Nagel) according to the manufacturer's protocol. RNA concentrations were measured spectrophotometrically and total RNA (300 ng) was reverse transcribed with High-Capacity cDNA Reverse Transcription Kit (Thermo Scientific, Waltham). qPCR was performed by using TaqMan™ Universal Master Mix II with UNG (Thermo Scientific) according to the manufacturer's instructions. The human IL-6 (Hs00985639), PTK2 (Hs01056457), MAP3K8/TPL2 (Hs00178297) and ACTB (Hs99999903_m1) TaqMan Gene Expression Assays (all from Applied Biosystems) were used in a StepOne Real-Time PCR engine (ThermoFisher). The relative gene expression was calculated using the comparative CT method.

ELISA

For the detection of IL6 secreted in the medium, HeLa cells were transfected with appropriate siRNAs for two rounds. 48 h after the second round cell supernatant was collected, centrifuged at 1.500 rpm for 10 min at 4 °C and probed for the presence of IL6 with the use of Human IL-6 Quantikine ELISA Kit (R&D Systems), according to providers' instructions.

Statistical analysis

Graphs were prepared using PRISM (Graphpad Software Inc.) or Microsoft Excel software and statistical significance was concluded based on one or two-way ANOVA as necessary using the SigmaStat 3.5 software.

Results

ERK signaling by inflammatory stimuli is compromised in ECM-detached cells

We compared the kinetics of ERK phosphorylation in adherent *versus* ECM-detached HeLa cervical carcinoma cells and immortalized mouse embryo fibroblasts (MEF) following exposure to TNF. As shown in a representative immunoblot in Fig. 1A and in Supplementary Fig. 1A, a defect in ERK but not JNK phosphorylation was observed in ECM-detached HeLa cells treated with TNF compared to adhered cultures. In detached MEFs, TNF stimulation also largely failed to induce phosphorylation of ERK1/2, compared to adhered cells (Fig. 1B). Similar results were obtained by monitoring ERK phosphorylation in ECM-adhered *versus* detached EJ bladder carcinoma cells exposed to recombinant soluble CD40L (Fig. 1C). We also utilized a mouse fibroblast cell line stably expressing CD40 [12] and we observed similar defects in MEK and ERK activation upon detachment from ECM (Fig. 1D). In contrast, HeLa cells exposed to EGF responded by activating ERK irrespective of adhesion to ECM (Suppl. Figure 1B).

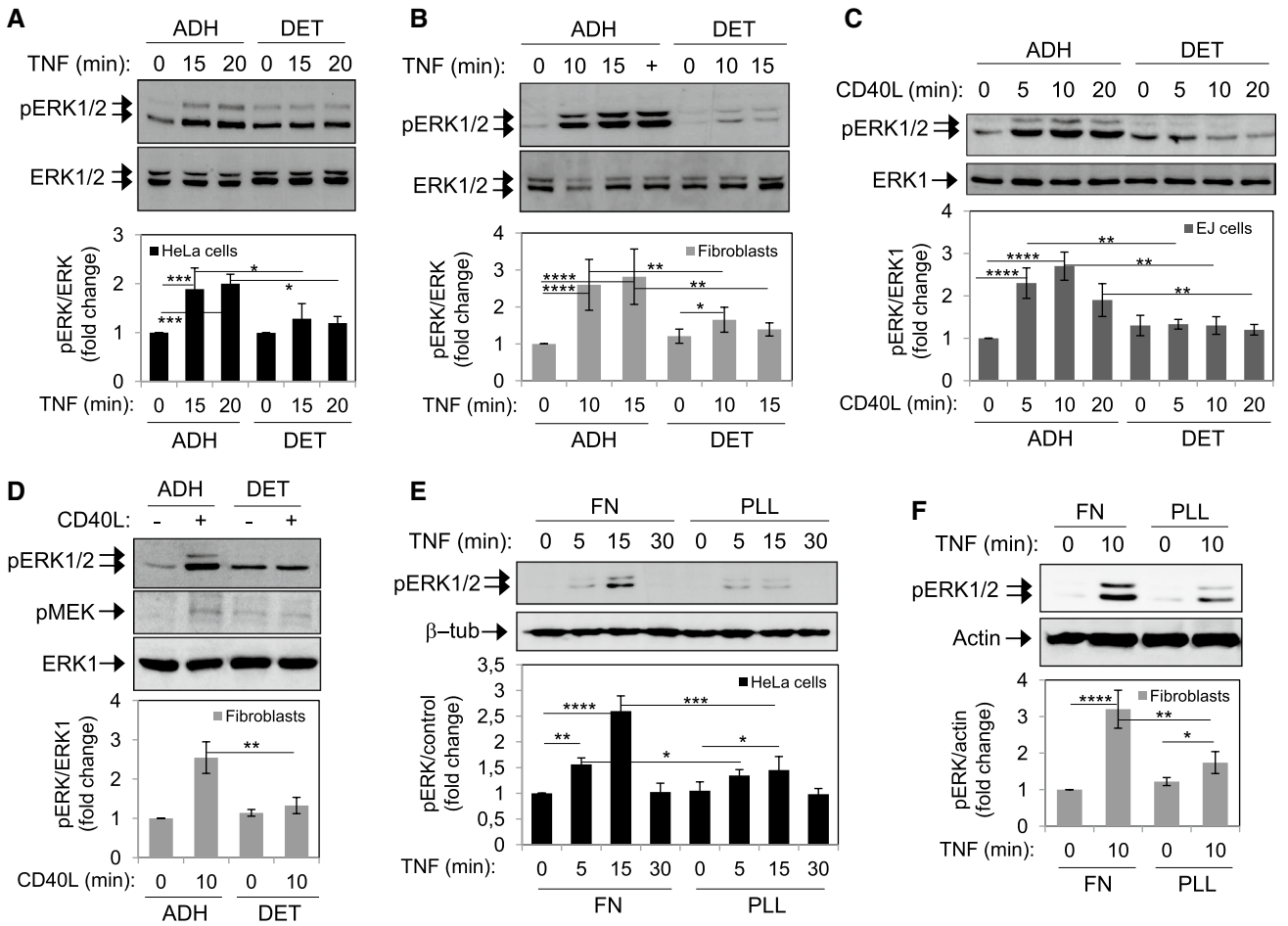

Fig. 1 Cell detachment attenuates TNF and CD40L-induced ERK activation. **A**–**D** HeLa cervical carcinoma cells and fibroblasts were detached from the culture plate and incubated in suspension for 3 or 2 h, respectively, prior to either re-plating (adherent, ADH) or continuation of culture under detached (DET) conditions for another hour. Cells were then stimulated with 50 ng/ml TNF (**A** & **B**) or 1 µg/ml recombinant trimeric CD40L (**C** & **D**) for various time intervals as indicated before lysis and assessment of ERK phosphorylation (p-ERK1/2) or loading controls by immunoblot. In (**B**), adherent fibroblasts were also stimulated with 10 ng/ml EGF for 5 min, which serves as positive control (+) for ERK phosphorylation. **E** & **F** HeLa cells *(E)* and fibroblasts *(F)* were suspended as described above and re-plated to either fibronectin (FN) or poly-L-Lysine (PLL) before stimulation with TNF and assessment of phosphorylated ERK by immunoblot. Densitometric quantification of p-ERK *versus* loading controls from at least three independent blots is shown in the lower part of each panel and two-way ANOVA was used to assess statistically significant differences (*$p<0.05$, **$p<0.01$, ***$p<0.001$)

We next examined if the aforementioned effects of cell detachment on inflammatory signal transduction are mediated by integrin receptor engagement. Integrin receptors comprise a superfamily of transmembrane proteins that are the major mediators of cell contacts with ECM components. To this end, we compared the effects of fibronectin which is recognized by α5β1 integrin, *versus* Poly-L-Lysine (PLL), a positively charged polypeptide that augments cell binding to the culture dish by enhancing electrostatic interactions with cell membranes without activating integrin-dependent signaling. HeLa cells and mouse fibroblasts were plated on either PLL or fibronectin, stimulated with TNF and examined for ERK phosphorylation at various time intervals. Similar to detached cells, ERK signaling was found to be compromised in the absence of integrin engagement (Fig. 1E, F). We conclude that cell attachment supports ERK signaling downstream of the TNF and CD40L receptors.

Cell detachment impacts TPL2 levels and activity

TPL2 is positioned downstream of various inflammatory pathways by directly activating MEK, the ERK kinase [15–17]. On the basis of the results shown in Fig. 1, we hypothesized defects in TPL2 activation in ECM-detached cells, which prompted us to investigate the levels and catalytic activity of TPL2 under these conditions.

First, we confirmed the involvement of TPL2 in ERK pathway activity downstream of CD40 and TNF activation in epithelial cells and fibroblasts. We knocked-down TPL2 in HeLa cells prior to treatment with TNF and assessed ERK

phosphorylation in cell lysates (Fig. 2A, B and Suppl. Figure 2). We also exposed HeLa cells (Fig. 2C, E) and fibroblasts (Fig. 2D, E) to a small molecule chemical inhibitor of TPL2 (TPL2i) and evaluated phosphorylated ERK levels before and after TNF stimulation. In all these cases, inhibition of TPL2 compromised TNF-induced ERK phosphorylation. Similar results were obtained in CD40L-stimulated EJ cells in which the kinase activity of TPL2 was ablated by treatment with the chemical inhibitor (Fig. 2F, G).

Next, we examined the impact of cell detachment on TPL2 expression levels. Differential translational initiation of the TPL2 mRNA gives rise to two isoforms, p58 (58 kDa) and p52 (52 kDa). In unstimulated cells, both isoforms are complexed with p105 NF-κB1 and ABIN2 and are protected from degradation. Upon cell treatment with an activation stimulus, p58 is preferentially released from p105 relative to the p52 isoform [14] to phosphorylate MEK1/2. Released p58 TPL2 is targeted by the E3 ubiquitin ligase SKP2 and the proteasome for degradation, thereby limiting the duration of MEK-ERK signal activation [20].

HeLa cells were cultured in suspension for 3 or 24 h and lysates were analyzed for TPL2 expression by immunoblot. Cell detachment was found to cause a time-dependent reduction in TPL2 p58 levels compared to adherent control cultures (Fig. 3A), in the absence of changes in TPL2 mRNA levels (Fig. 3B). Similarly, detached MEFs displayed a reduction in the steady-state levels of p58 TPL2 (Fig. 3C).

In line with the established model of TPL2-mediated ERK signal transduction [13], adherent MEFs stimulated with TNF displayed a progressive reduction in the endogenous TPL2 p58 levels whereas p52 TPL2 remained unaffected (Fig. 3C). In contrast, detached MEFs only partially responded to TNF

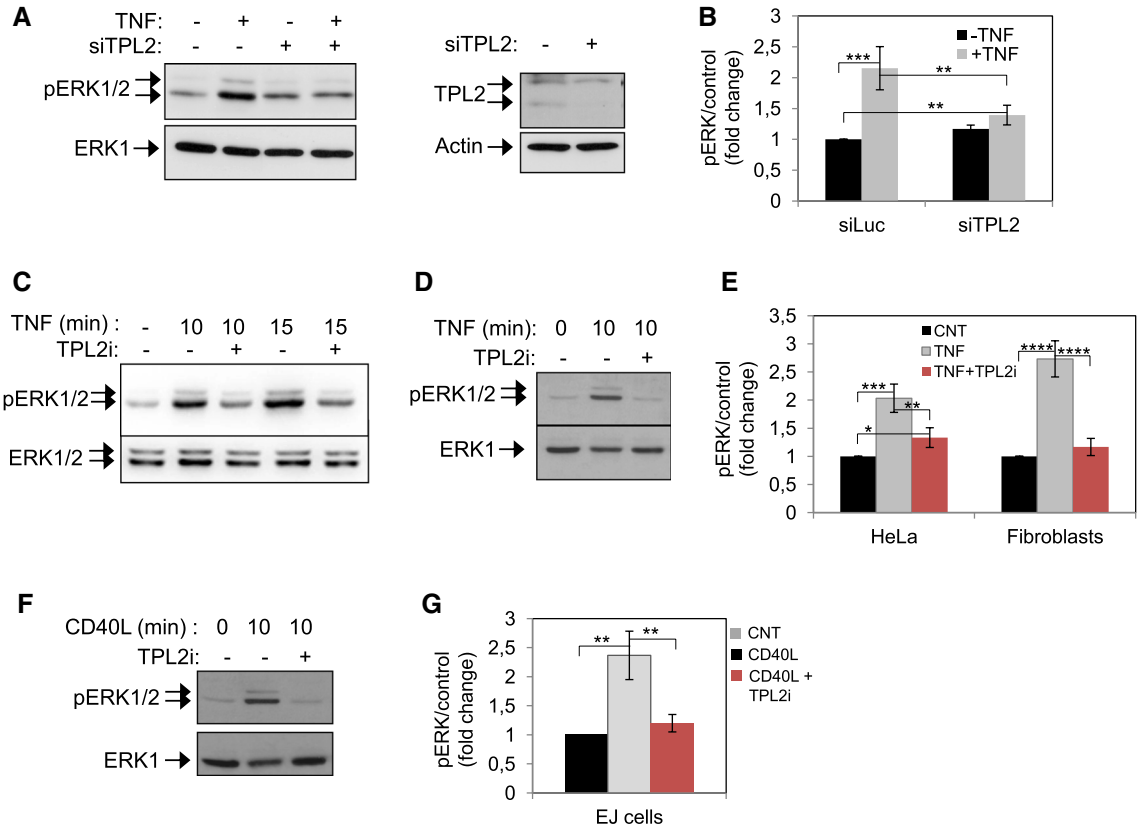

Fig. 2 TNF and CD40L-induced ERK phosphorylation in carcinoma cells and fibroblasts depends on the TPL2 kinase. **A** & **B** The knockdown of TPL2 attenuates TNF-induced ERK phosphorylation in HeLa cervical carcinoma cells. HeLa cells were transfected with siRNA targeting TPL2, followed by stimulation with 50 ng/ml TNF for 10 min. Untreated and TNF-treated cells were lysed and analyzed for expression of phosphorylated ERK1/2 by immunoblot in a representative experiment (left panel). The knockdown efficacy was confirmed by immunoblot using an anti-TPL2 Ab (right panel). Detection of ERK1 and β-actin levels was used as loading control, respectively. In (**B**), collective data from $n=3$ experiments are shown (**$p<0.01$, ***$p<0.001$ by two-way ANOVA). **C**–**E** Suppression of the catalytic activity of TPL2 by a small molecule chemical inhibitor (TPL2i) attenuates TNF-induced ERK phosphorylation in HeLa cells (**C** & **E**) and mouse fibroblasts (**D** & **E**). Cells were treated with 20 μM TPL2i, followed by TNF stimulation as described in (**A**). In (**E**), collective data from at least 3 experiments are shown (*$p<0.05$, **$p<0.01$, ***$p<0.001$, ****$p<0.0001$ by two-way ANOVA). **F** & **G** Treatment of EJ bladder carcinoma cells with 20 μM TPL2i attenuates CD40L-induced ERK phosphorylation. In (**G**), collective data from three experiments are shown in which cells were treated with 1 μg/ml CD40L for 10 min (**$p<0.01$, by two-way ANOVA)

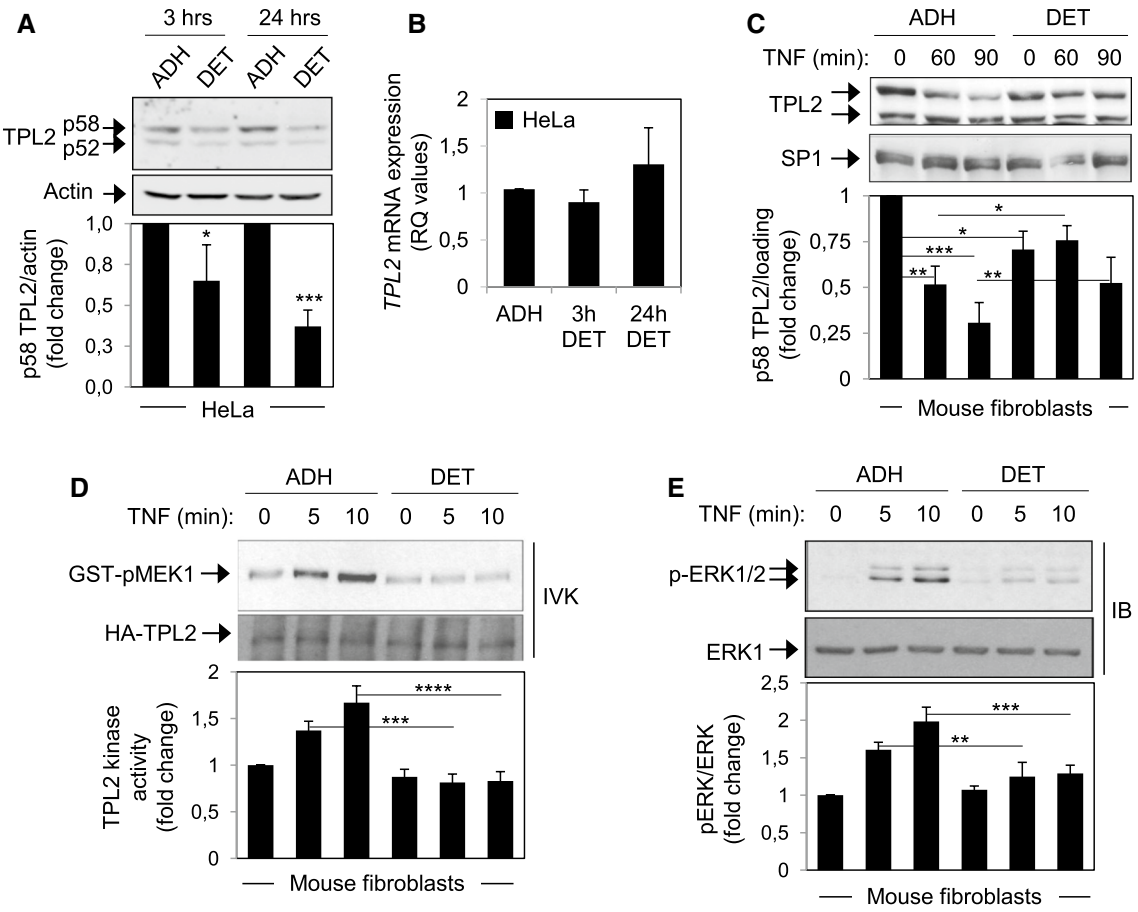

Fig. 3 Cells detached from ECM display defects in TPL2 expression and kinase activity. **A** Cell detachment impacts basal expression levels of TPL2. HeLa cells were cultured in the presence (ADH) or absence (DET) of adhesion to ECM for the indicated time points before lysis and assessment of endogenous TPL2 levels by immunoblot. The position of p58 and p52 isoforms of TPL2 is indicated. Quantification of p58 TPL2 versus the loading control was performed in 4 independent experiments and the results are shown in histogram form where expression in adhered cultures was given the arbitrary value of 1 ($*p<0.05$, $***p<0.001$). **B** Cell detachment does not affect *TPL2* mRNA levels. RNA was isolated from HeLa cells treated as in (**A**) and assessed for relative expression of *TPL2* by TaqMan qPCR. The results were normalized to the housekeeping β-actin gene and are expressed as RQ values. Differences in expression were not statistically significant by one-way ANOVA. **C** TNF stimulation of adherent (ADH) wild-type mouse fibroblast cultures results in progressive reduction in the endogenous p58 TPL2 levels whereas detached (DET) fibroblasts are partly responsive. Quantification of p58 TPL2 versus the loading control was performed in three independent experiments and the results are shown in histogram form; differences were statistically significant for ADH cultures stimulated with TNF versus untreated cells ($*p<0.05$, $**p<0.01$, $***p<0.001$ by two-way ANOVA). **D** & **E** $Tpl2^{-/-}$ mouse fibroblasts reconstituted to express HA-TPL2 at near physiological levels [14] were stimulated with TNF at either detached (DET) or adherent (ADH) state. Lysates were analyzed for TPL2 kinase activity against inactive GST-tagged MEK1 (in vitro kinase assays; IVK) as described in 'Materials & Methods' (*D*) or immunoblotted (IB) for p-ERK and ERK1 as loading control (*E*)

treatment by p58 TPL2 degradation (Fig. 3C), indicative of reduced TPL2 catalytic activity. This observation prompted us to directly assess TPL2 kinase activity downstream of TNFR1. To this end, we used MEFs from $tpl2^{-/-}$ mice transduced to express HA-tagged p58 TPL2 at physiological levels [14] and subjected them to TNF treatment before or after ECM attachment. HA-TPL2 was immunoprecipitated from cell lysates and assessed for catalytic activity in in vitro kinase assays using recombinant GST-MEK1 as substrate. Analysis of the resultant $Ser^{217/221}$-phosphorylated MEK1 demonstrated impairment of the enzymatic activity of TPL2 towards MEK in detached *versus* attached cells (Fig. 3D) which paralleled diminished ERK signaling in the detached cultures (Fig. 3E). We conclude that the levels and activity of TPL2 require input from integrin: ECM interactions.

Cell detachment mimics TPL2 inactivation in sensitizing carcinoma cells to death-inducing receptor ligands

Inhibition of ERK renders tumor cells sensitive to apoptosis induced by TNF and CD40L [2, 30] and the

combination of TPL2 knockdown and TNF treatment causes synthetic lethality in human carcinoma cells [26]. We herein extend these observations by showing that reduced catalytic activity of TPL2 sensitizes carcinoma cells to both TNF and CD40L-induced death. This was demonstrated by exposing HeLa cells to either TPL2i or, as a control, cycloheximide (CHX) to inhibit de novo protein synthesis of survival factors, followed by a 4 or 24 h treatment with TNF. As shown in Fig. 4A, B, the suppression of TPL2 kinase activity sensitized HeLa cells to TNF-induced apoptosis in a time-dependent manner. Combination treatment with TPL2i and CHX led to even more pronounced apoptotic effect compared to either inhibitor alone (Fig. 4B), indicative of additional signaling factors affecting the balance of TNF-induced apoptosis *versus* survival, such as NF-κB [31]. Similarly, the combination of TPL2i and CD40L treatment was found to cause synthetic lethality in CD40-transfected HeLa cells [2] which was augmented upon inhibition of de novo protein synthesis (Fig. 4C).

As detachment lowers basal TPL2 levels and leads to defects in TPL2-ERK signaling (Fig. 3), we asked whether cell detachment mimics the effects of TPL2 knockdown [26] or inactivation of its catalytic activity (Fig. 4A–C) in sensitizing carcinoma cells to death-inducing receptor ligands. To this end, we explored EJ bladder carcinoma cells, a CD40-positive cell line previously shown to respond to CD40 agonist-mediated killing in the presence of the protein synthesis inhibitor CHX [2]. Cells were detached from ECM and cultured in suspension in the presence of soluble trimeric CD40L or EGF for 24 h. Cell death was evaluated by SYTO^{TM}16/Propidium Iodide double staining and flow cytometry. Compared to untreated controls cultured in suspension, treatment with CD40L caused a significant, threefold increase in EJ cell death (Fig. 4D, E). In contrast to pro-inflammatory TNF family death ligands, treatment with the unrelated growth factor EGF did not increase apoptosis in detached cultures (Fig. 4D, E).

We conclude that disrupting the engagement of carcinoma cells to extracellular matrix mimics TPL2 inactivation

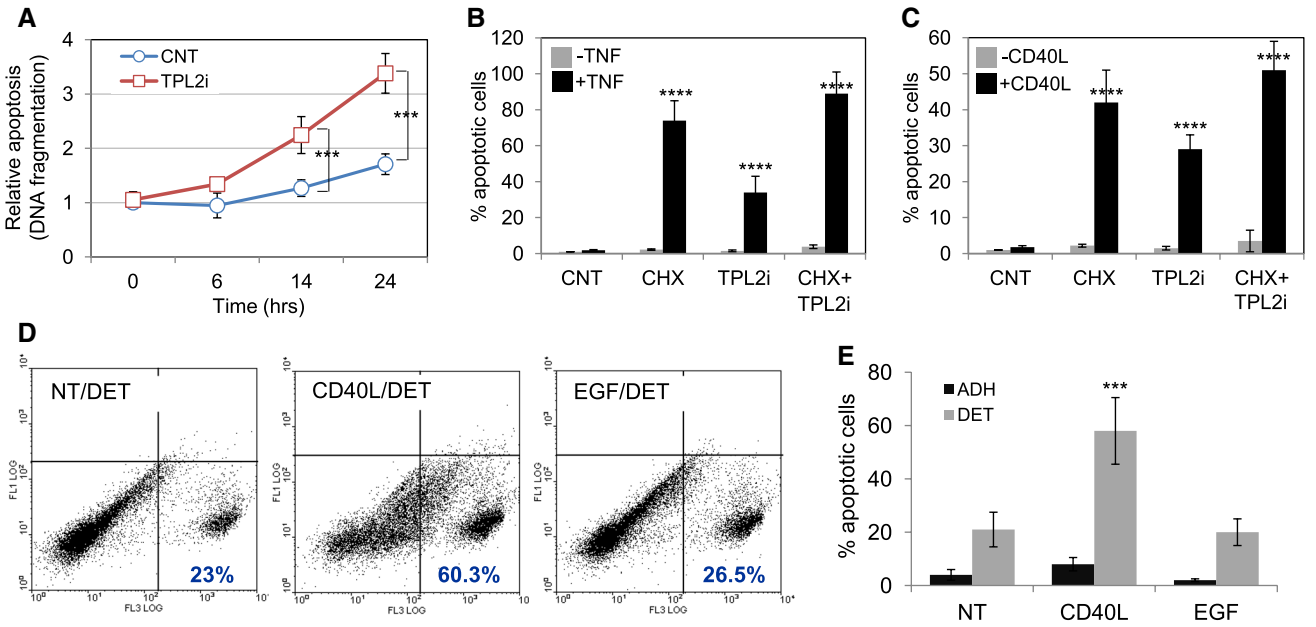

Fig. 4 Cell detachment mimics TPL2 inactivation in sensitizing carcinoma cells to death-inducing receptor ligands. **A** & **B** The combination of TPL2 inhibitor (TPL2i) and TNF treatment causes synthetic lethality in human carcinoma cells. In (**A**), HeLa cells were treated with 20 μM TPL2i in the presence or absence of 50 ng/ml TNF for 6, 14 or 24 h as indicated and apoptosis was assessed using a Cellular DNA Fragmentation ELISA. Two-way ANOVA confirmed statistically significant differences in TNF-stimulated cells treated with TPL2i *vs* vehicle control (CNT) ($n=3$; ***$p<0.001$). In (**B**), HeLa cells were treated with 20 μM TPL2i in the presence or absence of 50 ng/ml TNF for 24 h and the number of apoptotic cells were measured following PI staining and microscopy ($n=4$ independent experiments, mean ± SD is shown). TNF and CHX (5 μg/ml) combination treatment was used as control for the induction of cell death. **C** The combination of TPL2i and CD40L treatment causes synthetic lethality in CD40-expressing HeLa carcinoma cells. Treatments were performed as in (B). Quantification of apoptosis (measured by PI staining and microscopy) from three independent experiments is shown (mean ± SD). **D** & **E** Cell detachment sensitizes human carcinoma cells to CD40L-induced cell death. EJ cells were cultured in suspension (DET) in the presence of CD40L or EGF prior to analysis of cell death using Syto^{16} staining and flow cytometry. Untreated cultures (NT) were used as baseline control. A representative assay is shown in (**D**) and collective data from three experiments are shown in (**E**). The *y* axis represents propidium iodide and the *x* axis Syto^{16} staining. CD40L-induced cell death in detached cells was significantly different from the respective NT and EGF treatments (***$p<0.001$ by two-way ANOVA)

in sensitizing carcinoma cells to death-inducing receptor ligands.

Focal adhesion kinase sustains inflammatory TPL2-dependent ERK signal transduction in ECM-attached cells

Fibronectin, a focal adhesion-inducing integrin ligand, enables TNF-mediated ERK signaling whereas PLL which does not organize focal adhesions [32] impairs it (Fig. 1). Focal Adhesion Kinase (FAK) is activated in focal adhesions [33] and mediates anchorage-dependent survival signaling through integrin-dependent but also integrin-independent mechanisms, by interacting with RIPK1 [7]. Our previous work has shown that RIPK1 is required for TNFR1-mediated ERK signaling ([34] and Suppl. Figure 2) and FAK has been implicated in the regulation of inflammatory signal transduction through various mechanisms, including the interaction with TNFR1 and RIPK1 [35, 36]. Collectively, the aforementioned observations provided the rationale for examining the role of FAK in TPL2-ERK signaling.

To this end, HeLa cells were transfected with a pool of 4 siRNAs targeting *PTK2* (coding for FAK) or control siRNA and lysates were analyzed for FAK and TPL2 expression levels by immunoblot. The results (Fig. 5A, B) showed efficient depletion of FAK by si*PTK2* that was paralleled by reduced expression of TPL2 at the protein but not the RNA level. Accordingly, FAK depletion compromised ERK activation in HeLa cells stimulated with TNF (Fig. 5B, C and Suppl. Figure 2). Moreover, the stimulus-induced degradation of p58 TPL2 was revoked in FAK-depleted cells (Fig. 5B), denoting loss of TPL2 kinase activity.

The specificity of the *PTK2* knockdown effect on TNF-induced ERK activation was confirmed by rescue experiments using avian FAK. Chicken FAK escapes the RNAi machinery in the cell because it has base-pair mismatches with the siRNA oligonucleotides we have used; thus, our approach explores a naturally existing FAK which is

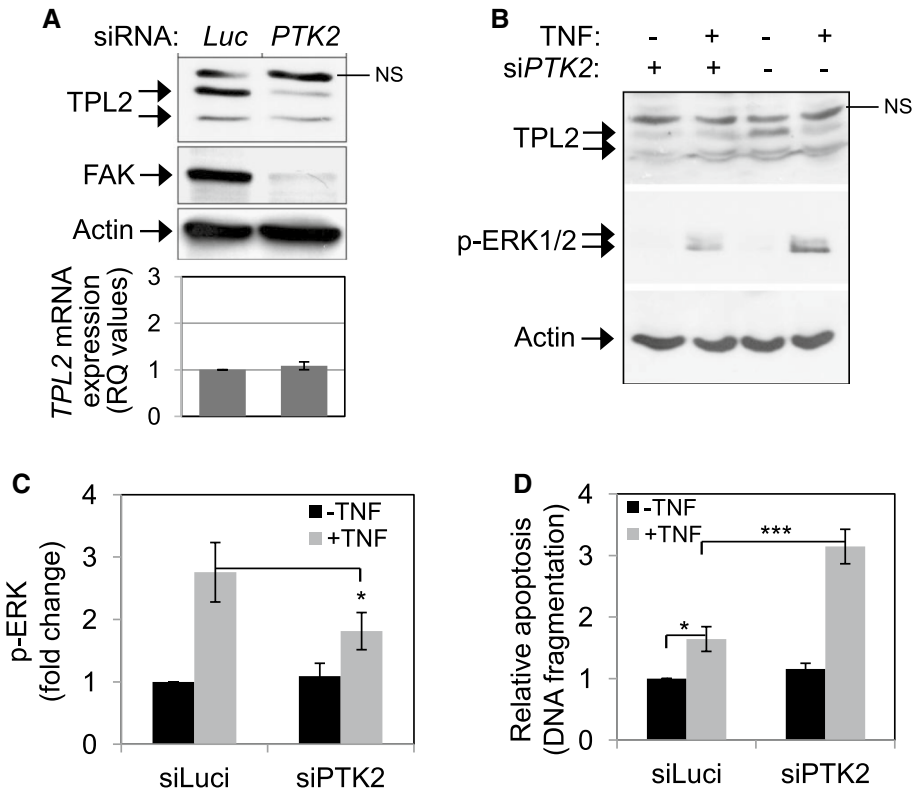

Fig. 5 Functional association of FAK with TPL2. **A** The knockdown of FAK results in reduced basal expression levels of TPL2. Lysates from FAK or control siRNA-transfected HeLa cells were immunoblotted for the indicated proteins. Parallel cultures were used for RNA isolation and assessment of *TPL2* mRNA levels by TaqMan qPCR (lower panel) and results were normalized to the housekeeping β-actin gene and expressed as RQ values. **B** The knockdown of FAK impacts the TPL2-ERK pathway. HeLa cells were transfected with either *PTK2* or control siRNA, and 24 h following the last round of knockdown they were exposed to 50 ng/ml TNF or left untreated. Lysates were immunoblotted for the indicated proteins. *NS;* non-specific. **C** Densitometric quantification of p-ERK versus loading controls from four independent experiments is shown for B (*$p < 0.05$ by two-way ANOVA). **D** The knockdown of FAK sensitizes HeLa carcinoma cells to TNF-induced apoptosis. Following transfection with either si*PTK2* or si*Luci,* HeLa cells were exposed to 50 ng/ml TNF (R&D Systems, 8599-TA) prior to assessment of apoptosis with a Cellular DNA Fragmentation ELISA

resistant to the human FAK siRNAs. Following endogenous *PTK2* knockdown, HeLa cells were co-transfected with a MYC epitope-tagged (MT) chicken FAK-expressing plasmid and HA-tagged ERK1 and 24 h later, cells were either left untreated or stimulated with 50 ng/ml TNF. Analysis of immunoprecipitated HA-ERK1 showed that exogenously expressed FAK enabled the activation of ERK under these conditions (Suppl. Figure 3).

As FAK is required for the effective activation of the TPL2-MEK-ERK axis in response to TNF, and both detachment and TPL2 inhibition sensitize carcinoma cells to TNF-induced apoptosis, we tested the hypothesis that FAK depletion may also render carcinoma cells susceptible to TNF-induced apoptosis. This was confirmed in HeLa cells following knockdown of *PTK2* and treatment with TNF, relative to control cultures (Fig. 5D).

FAK depletion activates the NF-κB/IL-6/STAT3 signaling pathway to upregulate the expression of the TPL2 E3 ubiquitin ligase SKP2.

The data presented in Fig. 5A, B implicate FAK in the post-transcriptional regulation of TPL2. As ubiquitin-mediated degradation represents a major post-transcriptional pathway controlling TPL2 expression levels, and SKP2 has been identified as a TPL2 E3 ubiquitin ligase [20], we postulated that FAK depletion may up-regulate SKP2. To address this hypothesis, HeLa cells were transfected with siRNAs targeting *PTK2*, *TPL2* or a control siRNA, RNA was isolated and *SKP2, PTK2* or *TPL2* expression levels were quantified by TaqMan qPCR. The results (Fig. 6A) showed specific knockdown of *PTK2* and *TPL2* by the respective siRNAs and a 1.8-fold increase of *SKP2* mRNA levels by the knockdown of *PTK2* (but not of *TPL2*) relative to control siRNA.

Previous studies have shown that *SKP2* is a direct transcriptional target of activated STAT3 [37–39]. Interestingly, we found that the knockdown of *PTK2* led to increased nuclear levels of Tyr^{705}-phosphorylated STAT3, a surrogate for STAT3 activation (Fig. 6B). We hypothesized that FAK may regulate STAT3 through the production of IL-6, a potent activator of STAT3 [40]. Indeed, the knockdown of *PTK2* led to elevated *IL6* mRNA levels, measured by TaqMan qPCR, whereas the knockdown of *TPL2* had no significant effect compared to control siRNA (Fig. 6C). To functionally validate this finding, we employed ELISA to quantify IL-6 in the supernatants of HeLa cell cultures transfected with si*PTK2* or control siRNA and confirmed elevated IL-6 levels in FAK-depleted cells (Fig. 6D). These culture supernatants were then applied to control HeLa cells and the phosphorylation status of STAT3 was examined at various time intervals. The results (Fig. 6E and Suppl. Figure 4) demonstrated increased phosphorylation of STAT3 in cells exposed to supernatant from FAK-depleted cultures relative to supernatant from control siRNA-transfected cells, in line with the presence of higher IL-6 levels in the former (Fig. 6D). Additional evidence implicating IL-6 in STAT3 phosphorylation is provided by data showing that pre-incubation of supernatant from FAK-depleted cultures with a neutralizing anti-IL-6 mAb prior to cell treatment led to reduced STAT3 phosphorylation (Fig. 6F).

Because *IL6* is transcriptionally regulated by RelA (p65) NF-κB [29], we tested the hypothesis that the knockdown of FAK induces NF-κB activation. Indeed, when an NF-κB-dependent promoter luciferase reporter plasmid (κBconA-Luc, [29]) was transfected into HeLa cells together with *PTK2* siRNA, we detected a 2–2.5-fold higher NF-κB transcriptional activity compared to control siRNA-transfected cells (Fig. 6G). This observation aligns with the elevated levels of RelA p65 detected in nuclear extracts isolated from FAK-depleted HeLa cells *versus* control cultures (Fig. 6H). The generality of these findings was confirmed in A549 lung cancer cells where the knockdown of *PTK2* led to increased nuclear accumulation of RelA and higher NF-κB transcriptional activity compared to control siRNA (Suppl. Figure 5). We also observed that the RNAi-mediated depletion of FAK resulted in reduced levels of both IκBα and p105 NF-κB1, denoting elevated IKK activity (Fig. 6H).

Collectively, these data suggest that FAK depletion activates the IκB/NF-κB signaling pathway that may impact TPL2 expression via (a) reduction in p105 NF-κB1 levels that control TPL2 stability [41] and (b) the activation of the IL-6/STAT3 axis that upregulates the expression of SKP2, a TPL2 E3 ubiquitin ligase [20].

cIAP2 is regulated by FAK and modulates FAK-dependent IKK/NF-κB signaling.

It has been reported that cIAP2 and RIPK1 are required for optimal TNF-induced cytokine and chemokine production [42]. The cellular effects of RIPK1 depend on its ubiquitination status which is dictated by the ubiquitin ligases cIAP1 and cIAP2 that directly bind RIPK1. The cIAP-mediated conjugation of K63-linked polyubiquitin chains to RIPK1 enables its association with the prosurvival kinase TAK1 and the activation of NF-κB and MAPK signaling [43]. NF-κB upregulates the expression of cIAP2, further increasing TNFR1 complex stability and pro-survival signaling. These observations provided the rationale for testing the physical and functional association of FAK with the RIPK1/cIAP axis.

In line with this hypothesis, we found that *PTK2* knockdown leads to elevated levels of cIAP2 (Fig. 7A & histogram of Fig. 7C) which is abolished by treatment with the cIAP1/2 antagonist (SMAC mimetic) LBW242 (Fig. 7A). The upregulation of cIAP2 by FAK depletion was also evident at the RNA level (Fig. 7B) and was found to be mediated via

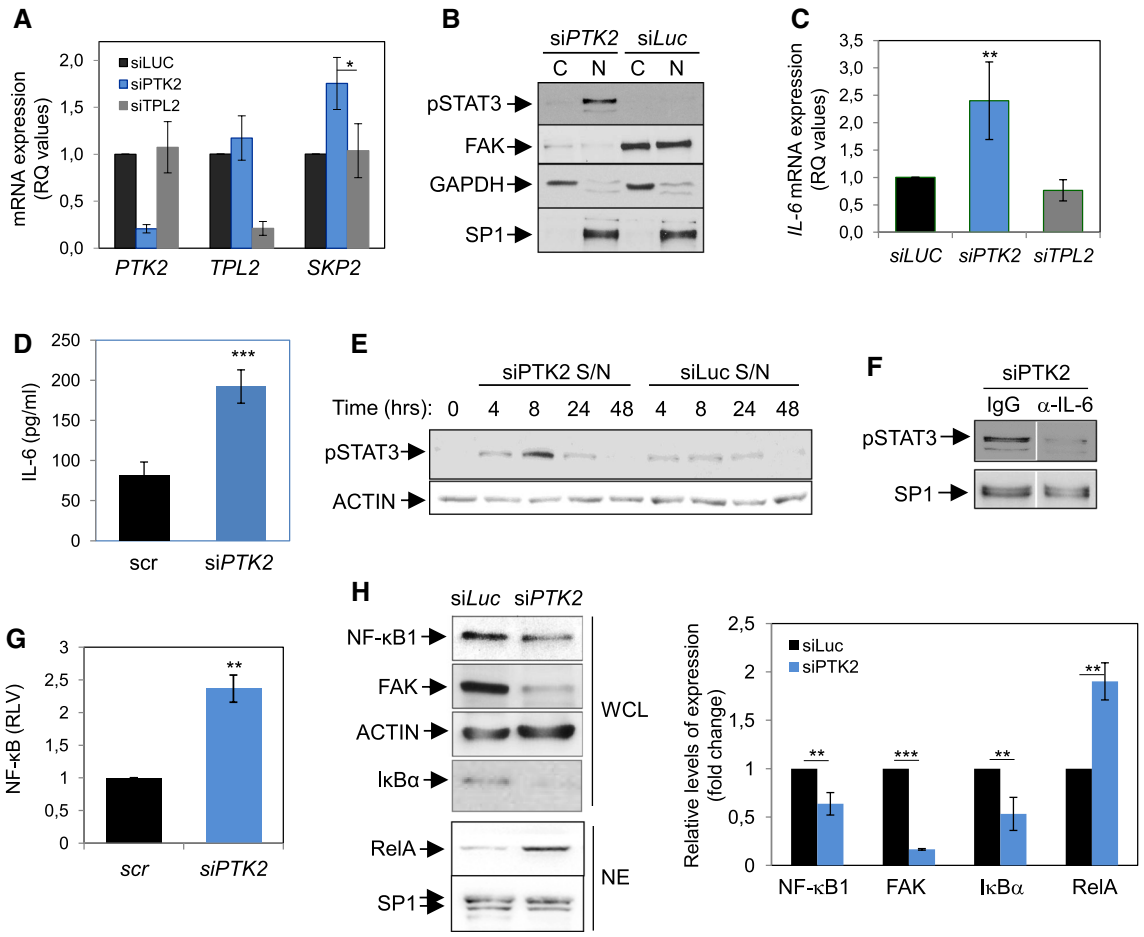

Fig. 6 Depletion of FAK modulates regulatory components of TPL2 **(A)** Up-regulation of *SKP2* expression by *PTK2* knockdown. HeLa cells were transfected with siRNAs targeting *PTK2* (si*PTK2,* blue bar) or *TPL2* (grey bar) or with a control siRNA (black bar), RNA was isolated and assessed for *PTK2, TPL2* or *SKP2* mRNA levels by TaqMan qPCR. The results were normalized to the housekeeping β-actin gene and expressed as RQ values (*y* axis). The data shown are the average from 4 independent experiments. **B** Nuclear accumulation of phosphorylated STAT3 (pSTAT3) upon knockdown of *PTK2*. GAPDH and SP1 were used as markers for the purity of cytoplasmic and nuclear protein extracts, respectively, and as loading controls. **C** The knockdown of *PTK2* results in the up-regulation of *IL-6* expression. HeLa cells were transfected with siRNAs targeting *PTK2* (blue bar) or *TPL2* (grey bar) or with a control siRNA (black bar), RNA was isolated and assessed for *IL-6* mRNA levels by TaqMan qPCR normalized to the housekeeping β-actin gene. **D** The knockdown of *PTK2* results in elevated secretion of IL-6, measured by ELISA. Student's *t* test was used to assess statistical significance, $***p < 0.001$. **E** & **F** Supernatants from si*PTK2 versus* control siRNA-transfected cells were used to culture HeLa cells for the indicated time points prior to assessment of phospho-STAT3 levels by immunoblot (**E**). Prior treatment of si*PTK2* supernatant with neutralizing IL-6 antibody reduced STAT3 phosphorylation (**F**). The results from multiple experiments were quantified and summarized in histogram form in Suppl. Figure 4. **G** The knockdown of *PTK2* results in the activation of NF-κB transcriptional activity, measured by luciferase reporter assays, as described in the Materials and Methods section. Student's *t* test was used to assess statistical significance, $**p < 0.01$. *RLV*: relative luciferase values. **H** The knockdown of *PTK2* results in reduced levels of NF-κB1 and IκBα proteins relative to control siRNA transfected cells, indicative of IKK activation. Analysis of nuclear extracts (NE) from parallel cultures identified higher levels of RelA NF-κB. SP1 and β-Actin serve as loading controls for nuclear and whole cell lysates (WCL), respectively. The results were quantified from three independent experiments and Student's *t* test was used to assess statistical significance in each pair, $**p < 0.01$, $***p < 0.001$

NF-κB because it was abolished by the simultaneous knockdown of *RELA* at both protein and RNA level (Fig. 7C, D).

We next examined the influence of cIAP2 on the FAK/IL-6/STAT3 axis. The RNAi-mediated knockdown of *cIAP2* abolished STAT3 phosphorylation caused by FAK depletion (Fig. 7E). As a complementary approach, we cultured FAK-depleted HeLa cells with LBW242 and found reduced levels of Tyr^{705} phosphorylated STAT3 (Fig. 7G). Moreover, the dual knockdown of *PTK2* and *cIAP2* resulted in lower secretion of IL-6 relative to FAK depletion alone (Fig. 7G). Collectively, these data implicate cIAP2 in IL-6/STAT3 signaling in FAK-depleted cells.

Because RIPK1 has a major role in NF-κB activation by TNF [43] and other stimuli [3, 44], and directly binds both FAK [7] and cIAPs [43], we examined the effects of *PTK2* knockdown on RIPK1:cIAP1/2 interactions. Cell lysates

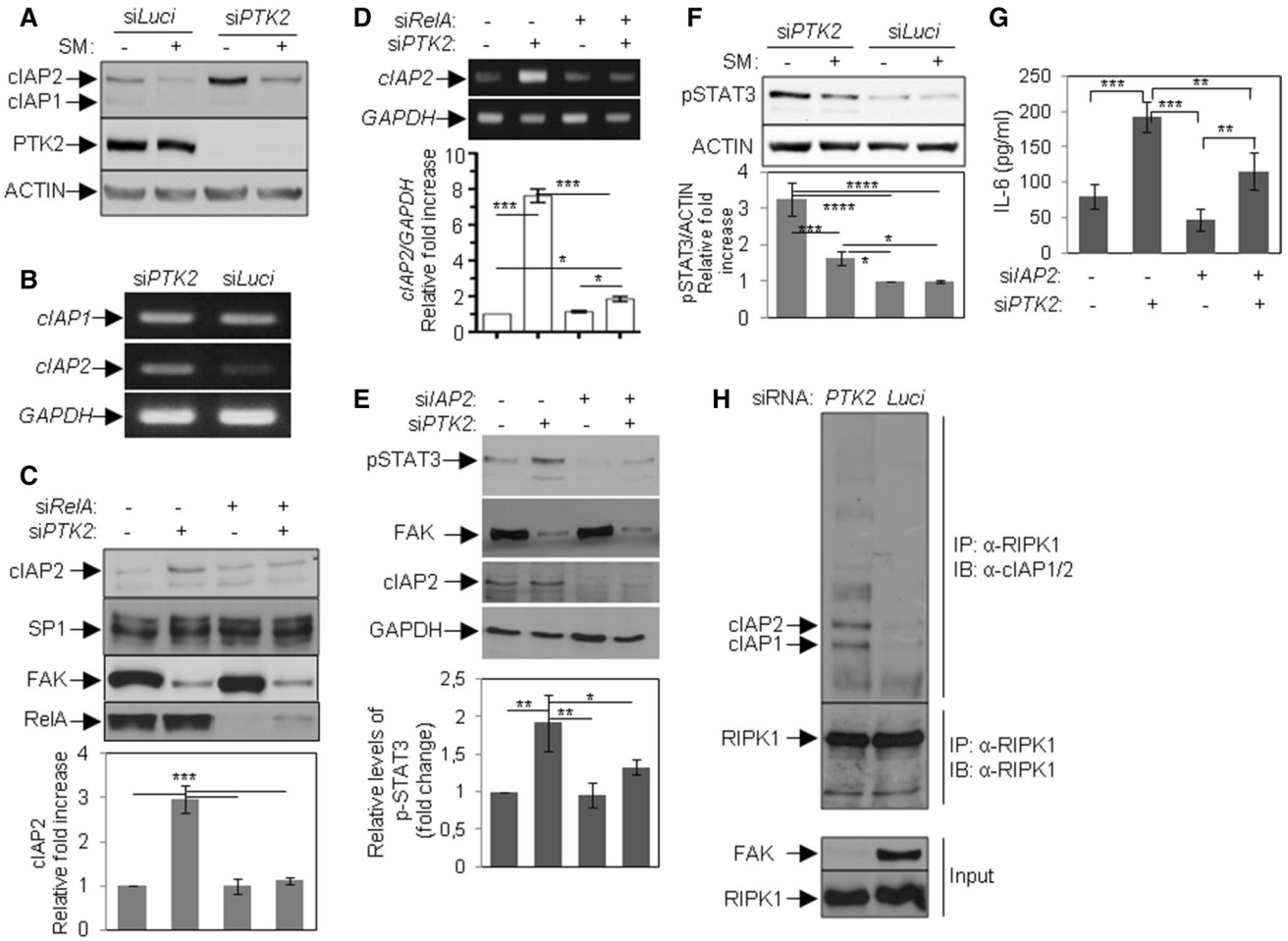

Fig. 7 Involvement of cIAP2 in the FAK/IL-6/STAT3 axis. **A** & **B** The knockdown of *PTK2* in HeLa cells up-regulates the expression of cIAP2 at the protein (**A**) and RNA level (**B**). The specificity of cIAP2 up-regulation is confirmed by cell treatment with the SMAC mimetic (SM) (cIAP antagonist) LBW242, as previously described [3]. **C** Involvement of RelA NF-κB in cIAP2 up-regulation upon FAK depletion. HeLa cells were transfected with si*PTK2,* si*RelA*, or their combination prior to lysis and analysis of cIAP levels by immunoblot, as indicated. Assessment of SP1, FAK and RelA levels serve as relevant controls. The relative expression levels of cIAP2 are shown in the lower panel histogram and two-way ANOVA was used to assess statistical significance (***$p < 0.001$ relative to any other treatment). **D** The knockdown of *RelA* abolishes *cIAP2* transactivation upon FAK depletion. The relative expression of *cIAP2* normalized to *GAPDH* was quantified and shown as graph. **E** & **F** cIAP2 is involved in STAT3 activation upon FAK depletion. In (**E**), HeLa cells were transfected with si*PTK2,* si*IAP2*, or their combination prior to lysis and analysis of pSTAT3 levels by immunoblot, as indicated. Assessment of FAK, cIAP2 and GAPDH levels serve as relevant controls. In (**F**), HeLa cells were transfected with si*PTK2* or control siRNA prior to treatment with SMAC mimetic (SM) LBW242 and assessment of pSTAT3 levels by immunoblot. Signals were quantified and the ratio pSTAT3/β-Actin is presented as graph. Two-way ANOVA was used to assess statistical significance (*$p < 0.05$, **$p < 0.01$, ***$p < 0.001$, ****$p < 0.0001$). **G** cIAP2 is involved in IL-6 secretion caused by depletion of FAK. HeLa cells were transfected as in (E) and culture supernatants were analyzed for IL-6 levels by ELISA. The data are the average of 4 independent assays. Two-way ANOVA was used to assess statistical significance between samples; ***$p < 0.001$; **$p < 0.01$. **H** The knockdown of *PTK2* increases the interaction of cIAPs with RIPK1. HeLa cells were transfected with si*PTK2,* or siRNA against the unrelated Luciferase (Luc) gene, lysed and immunoprecipitated (IP) with anti-RIPK1. Immunoprecipitates were then immunoblotted (IB) for cIAP1/2 or RIPK1, as indicated. Whole cell lysates (5% input) were used for immunoblotting as shown in the lower panel

from HeLa cells transfected with si*PTK2* or control siRNA were immunoprecipitated using an anti-RIPK1 antibody and immunoblotted for either cIAP1/2 or RIPK1. The results demonstrated increased association of cIAPs with RIPK1 upon FAK depletion (Fig. 7H). This observation aligns with the aforementioned effects of FAK depletion on the NF-κB/IL-6/STAT3 axis. The functional interplay between FAK and cIAPs is corroborated by the observation that LBW242 synergizes with FAK knockdown to amplify HeLa and A549 cell death (Suppl. Figure 6).

Discussion

Adhesion to extracellular matrix (ECM) influences a broad range of biological functions in nontransformed cells as well as several hallmarks of malignancy by facilitating cell survival, tumor growth, tumor evolution and metastasis [45]. It is envisaged that several of these adhesion-mediated properties impinge on other signaling pathways at multiple levels [46–48]. The data shown in this study confirm this prediction and demonstrate that the activation of ERK signaling by TNF or CD40L depends on the integrity of integrin:ECM interactions. Thus, cell detachment or integrin-independent adhesion to poly-L-lysine reduces the magnitude of MEK-ERK activation in carcinoma cells and immortalized fibroblasts exposed to TNF or CD40L (Fig. 1). We have mapped this defect at the level of TPL2, a MEK kinase with an obligatory role in TNFR1 and CD40-mediated ERK signal transduction ([12] and Fig. 2). Indeed, both the basal protein levels and the stimulus-induced catalytic activity of TPL2 are reduced in detached cells (Fig. 3) or upon depletion of FAK, a key component of integrin-mediated signal transduction (Fig. 5).

The expression levels and activation of TPL2 are known to be influenced by components of the NF-κB pathway, including p105 NF-κB1 which physically sequesters TPL2 in a stable but inactive state [41], and the IκB kinase β (IKKβ) which phosphorylates both NF-κB1 and TPL2 triggering their dissociation and enabling TPL2 catalytic activity [16]. The p58 isoform of TPL2 is preferentially released from p105 NF-κB1 to phosphorylate MEK1/2 [14] but is also targeted by the proteasome, thereby limiting the duration of MEK-ERK activation. SKP2 has recently been identified as an E3 ubiquitin ligase targeting p58 TPL2 for degradation [20].

As FAK knockdown impacts TPL2 levels and kinase activity (Fig. 5), we explored the possibility that components of the aforementioned TPL2 regulatory pathway are modulated by FAK. We have herein identified p105 NF-κB1 and SKP2 as relevant targets of FAK signaling. We showed that transient depletion of FAK endows the activation of the IKK/NF-κB axis which transactivates *IL-6*. In turn, the enhanced production of IL-6 leads to higher levels of activated STAT3 and its transcriptional target, *SKP2* [37–39] (Fig. 6). FAK depletion also reduces the levels of p105 NF-κB1, presumably through the IKK-mediated NF-κB1 phosphorylation that triggers its proteolytic processing [49]. On the basis of these observations we propose that FAK depletion impacts TPL2 levels by both upregulating SKP2 expression and reducing p105 NF-κB1 levels (Fig. 8).

Mechanistically, our observations align with recent evidence suggesting that disruption of focal adhesion kinase signaling may be associated with enhanced production of cytokines and chemokines. Thus, FAK ablation in cancer-associated fibroblasts (CAFs) leads to upregulation of several chemokine ligands with tumor-promoting potential which was only partly mimicked by a chemical inhibitor targeting the catalytic activity of FAK, indicating bifurcation of FAK kinase and nonkinase activities [10]. Interestingly, increased phosphorylation of STAT3 is observed in cancer cells exposed to FAK-depleted CAF conditioned media [10]. Moreover, detachment of carcinoma cells from the ECM has been associated with up-regulation of IL-6 expression [50], reminiscent of the effect of *PTK2* knockdown on IL-6 levels in carcinoma cells (Fig. 6) and of the increased secretion of IL-6 in FAK inhibitor-treated macrophages [51]. Other studies have shown that treatment of pancreatic tumors with FAK inhibitor rapidly eliminates CAFs, causing reduced intratumoral levels of TGF-β with concomitant STAT3 activation in malignant cells which enables them to resist inhibitor therapy [52].

FAK is overexpressed in several tumor types and attenuation of FAK signaling is considered a major therapeutic goal in cancer [53]. However, a closer look at the available evidence suggests significant variation in FAK expression both within a tumor and between primary tumors and their metastases. For example, expression of FAK in the stroma of breast and pancreatic tumors differs among patients and low stromal expression of FAK is associated with reduced overall patient survival [10]. Variations in FAK expression levels have also been reported in patients with cervical cancer where weak expression of FAK has been correlated with lymph node metastasis, recurrent disease and poor prognosis [54]. Similarly, low level of FAK expression in intrahepatic cholangiocarcinoma has been correlated with large tumor size and poor differentiation [55]. Significantly reduced levels of FAK have also been noted in liver metastases of colon adenocarcinomas compared to the primary tumors [56] and in melanoma cells derived from peripheral blood compared to matched primary melanomas [57]. Colon cancer cells at the migrating front of monolayer cultures also exhibit reduced total and activated FAK [58]. Our analysis of single cell transcriptomic data registered in the Broad Institute Single Cell Portal (https://singlecell.broadinstitute.org/single_cell) supports the heterogeneous nature of *PTK2* expression in triple negative breast cancer (TNBC) and colorectal tumors (Suppl. Figures 7 and 8). Thus, in TNBC, high *PTK2* expression was detected in subpopulations of malignant epithelial cells, cancer-associated fibroblasts and perivascular-like (PVL) cells but was expressed at very low levels in myeloid, B and T cells. The expression of *SKP2* was also heterogeneous and, interestingly, was found to be reversely correlated with that of *PTK2* inasmuch as the majority of cells expressing high levels of *SKP* possess very low levels of *PTK2* and

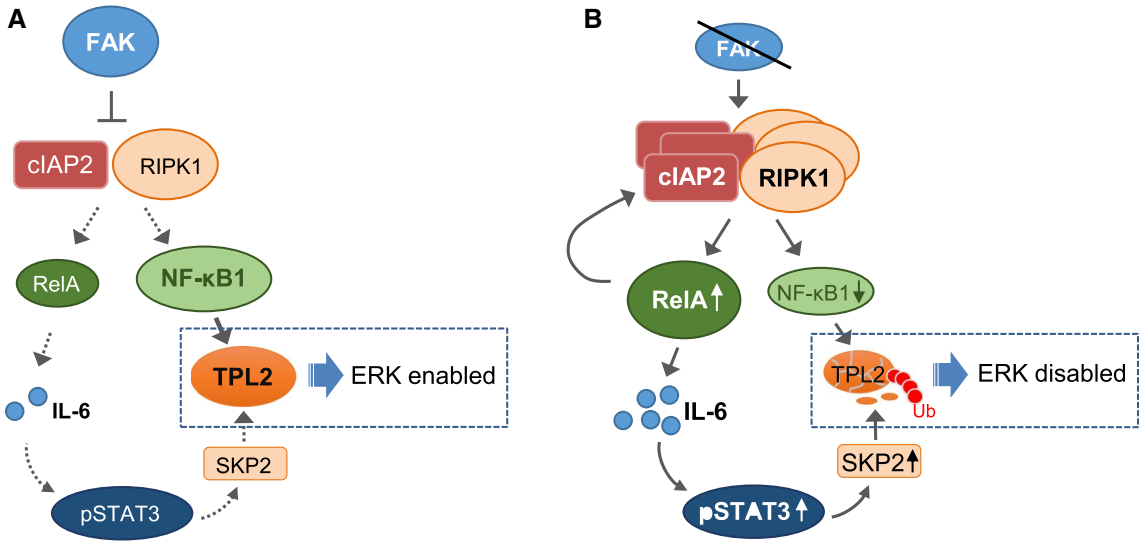

Fig. 8 Proposed mechanism by which cell adhesion may intersect pro-inflammatory TPL2 signaling. On the basis of the results presented herein we propose that Focal Adhesion Kinase (FAK) enables pro-inflammatory ERK signaling by modulating TPL2 expression and function. **A** In adhered cultures bearing physiological levels of FAK, RIP kinase 1 (RIPK1) minimally interacts with cIAP2, restricting signaling on the IκB kinase (IKK)-NF-κB axis. As a result, RelA transcriptional activity is low (dotted arrows) and, in the absence of IKK-mediated p105 NF-κB1 proteolysis, the entire TPL2 pool is complexed with NF-κB1 and stabilized (solid arrow). This TPL2 pool enables activation of MEK-ERK signaling in response to pro-inflammatory factors such as TNF and CD40L. **B** When cells are detached or FAK levels are reduced, as seen in certain types of malignancy or malignant cell populations (see Discussion), RIPK1:cIAP2 interactions increase, leading to reduced TPL2 expression levels by a dual mechanism. First, the activation of RelA NF-κB downstream of RIPK1:cIAP2 endows *IL-6* transactivation and elevated secretion of IL-6 that induces STAT3 activation (solid arrows). STAT3 is an established transcriptional activator of *SKP2* which encodes a TPL2 ubiquitin ligase. Second, the reduction in p105 NF-κB1 levels, which is known to occur through IKK-mediated phosphorylation and proteolysis [41], limits the stable TPL2 pool available to enable ERK activation upon TNF or CD40L stimulation. The activation of RelA also elevates the expression of cIAP2 that feeds back to RIPK1 to sustain IKK-NF-κB signaling. Interfering with nodal components of this pathway, such as FAK, cIAP2 and TPL2, provides opportunities for synthetic lethal interactions in cancer therapy or augmentation of the antitumor effects of TNF and CD40L. *Ub; ubiquitin*

vice versa (Suppl. Figure 7). A similar phenomenon was noted in colon cancer cell populations (Suppl. Figure 8). Collectively, the aforementioned published evidence and the results of our data mining support the in vivo relevance of the mechanistic data presented herein.

It is thus conceivable that low levels of FAK expression may not only have direct effects on the survival, migratory and/or angiogenic capacity of malignant or nonmalignant cells in the tumor microenvironment but could also impact tumor growth indirectly, for example through suppression of TPL2 expression and activity. Indeed, signaling by mutated RAS suppresses both FAK activity [11] and TPL2 expression levels [21] and reduced TPL2 has been associated with poor prognosis of lung cancer patients and more aggressive development of chemical-induced lung adenocarcinomas in the mouse [21]. We thus speculate that reduced expression of TPL2 in CAFs or malignant cells may contribute to the tumor-promoting effects of FAK depletion in vivo. The functional link between FAK and TPL2 is corroborated by a previous study showing that proteinase-activated receptor 1 (PAR1) transduces TPL2 signals that phosphorylate and activate FAK and enable cell migration [59]. Therefore, FAK and TPL2 form circuits which operate in various settings to modulate tumor growth.

However, we also note that tumors bearing reduced levels of FAK may become more susceptible to the cytotoxic effects of TNF family ligands, along the lines of the 'synthetic lethality' concept in cancer therapy. Indeed, both published evidence [60] and our data (Fig. 5D) suggest that ablation of FAK results in heightened sensitivity to apoptosis ensued by TNF. Reduced levels or activity of TPL2 reproduces the si*PTK2* phenotype and tilts the balance between TNF or CD40L-induced survival and death signals towards apoptosis (Fig. 4). The data presented herein also demonstrate that disruption of focal adhesions sensitize malignant epithelial cells to CD40-mediated death. We have previously reported that the pro-apoptotic properties of CD40 agonists in adhered carcinoma cells are partly counteracted by the parallel stimulation of the ERK pathway [2]. It is therefore likely that the sensitizing effects of detachment on CD40L-induced cell death result from diminished ERK activation (Figs. 1 and 2). However, a TPL2-dependent but ERK-independent contribution to this phenomenon cannot be excluded in light of the reported direct effects of TPL2 on preventing TNF-induced

caspase-8 activation [26] and the involvement of caspase-8 also in CD40-mediated death [3]. Irrespective of the precise mechanisms involved, the aforementioned observations suggest that the FAK-TPL2 axis could be explored for synthetic lethal interactions with TNF family members.

We also identified cIAP2 as a proximal modulator of FAK signaling impacting NF-κB-mediated IL-6 synthesis and STAT3 activation. cIAP2 directly binds RIPK1 and catalyzes the conjugation of K63-linked polyubiquitin chains that enable RIPK1 to serve as a pro-survival signaling platform. By degrading cIAPs, SMAC mimetics force RIPK1 de-ubiquitination and switch RIPK1 from a pro-survival scaffold to a caspase-8-activating complex that may operate independently from death receptors [43, 61, 62]. We have shown that FAK knockdown increases both cIAP2 levels and the formation of cIAP2:RIPK1 complexes (Fig. 7), suggesting that carcinoma cells depleted of FAK explore the cIAP2-RIPK1 survival axis to resist cell death. We propose that 'addiction' to this pathway could be therapeutically explored and predict that the relative increase in cIAP2:RIPK1 complexes may render FAK-depleted cells susceptible to formation of extended proapoptotic complexes following degradation of cIAPs. Indeed, the data presented herein demonstrate that cells bearing low levels of FAK are exquisitely sensitive to SMAC mimetic-induced death (Suppl. Figure 6).

Overall, we have herein uncovered a novel mode of regulation of inflammatory ERK signal transduction by adhesion-related molecules. Our data position TPL2 as a central mediator of pro-survival signaling downstream of TNF family receptors, which is preserved by active integrin-dependent signal transduction. The functional link between TPL2 and FAK underscores important contributions to cell fate decisions at the crossroad of inflammation and cancer with significant potential for the development of novel therapeutic concepts and synthetic lethal strategies in cancer.

Supplementary Information The online version contains supplementary material available at https://doi.org/10.1007/s00018-022-04130-7.

Acknowledgements We would like to thank Dr. George Gouridis (Foundation of Research & Technology Hellas, Crete) for critical reading of the manuscript, useful discussions, as well as or providing reagents, antibodies and expertise on protein biochemistry when needed. We would like to thank all current and previous members of Eliopoulos laboratory for sharing protocols, reagents, expertise and for useful discussions.

Author contributions MV: conceptualization, investigation, data collection and analysis, preparation of the original draft manuscript. K.G.: investigation, data collection and analysis; E.I.A: investigation, data collection and analysis; AGE: conceptualization, investigation and preparation of the final version of the paper. All authors critically reviewed and approved the final version.

Funding The project was realized using funds from European Commission (EC) Research Program INFLA-CARE (EC Contract 223151) granted to A.G.E.

Availability of data and material All relevant data are within the manuscript and Supplementary Information Appendix.

Declarations

Conflict of interest None to declare.

References

1. Micheau O, Tschopp J (2003) Induction of TNF receptor I-mediated apoptosis via two sequential signaling complexes. Cell 114:181–190
2. Davies CC, Mason J, Wakelam MJ, Young LS, Eliopoulos AG (2004) Inhibition of phosphatidylinositol 3-kinase- and ERK MAPK-regulated protein synthesis reveals the pro-apoptotic properties of CD40 ligation in carcinoma cells. J Biol Chem 279:1010–1019
3. Knox PG, Davies CC, Ioannou M, Eliopoulos AG (2011) The death domain kinase RIP1 links the immunoregulatory CD40 receptor to apoptotic signaling in carcinomas. J Cell Biol 192:391–399
4. Vardouli L, Lindqvist C, Vlahou K, Loskog AS, Eliopoulos AG (2009) Adenovirus delivery of human CD40 ligand gene confers direct therapeutic effects on carcinomas. Cancer Gene Ther 16:848–860
5. Paoli P, Giannoni E, Chiarugi P (2013) Anoikis molecular pathways and its role in cancer progression. Biochem Biophys Acta 1833:3481–3498
6. Hanahan D, Weinberg RA (2011) Hallmarks of cancer: the next generation. Cell 144:646–674
7. Kurenova E, Xu LH, Yang X, Baldwin AS Jr, Craven RJ, Hanks SK et al (2004) Focal adhesion kinase suppresses apoptosis by binding to the death domain of receptor-interacting protein. Mol Cell Biol 24:4361–4371
8. Golubovskaya VM (2010) Focal adhesion kinase as a cancer therapy target. Anticancer Agents Med Chem 10:735–741
9. Zhou J, Yi Q, Tang L (2019) The roles of nuclear focal adhesion kinase (FAK) on Cancer: a focused review. J Exp Clin Cancer Res 38:250
10. Demircioglu F, Wang J, Candido J, Costa ASH, Casado P, de Luxan DB et al (2020) Cancer associated fibroblast FAK regulates malignant cell metabolism. Nat Commun 11:1290
11. Zheng Y, Lu Z (2009) Paradoxical roles of FAK in tumor cell migration and metastasis. Cell Cycle 8:3474–3479
12. Eliopoulos AG, Wang CC, Dumitru CD, Tsichlis PN (2003) Tpl2 transduces CD40 and TNF signals that activate ERK and regulates IgE induction by CD40. EMBO J 22:3855–3864
13. Vougioukalaki M, Kanellis DC, Gkouskou K, Eliopoulos AG (2011) Tpl2 kinase signal transduction in inflammation and cancer. Cancer Lett 304:80–89
14. Cho J, Tsichlis PN (2005) Phosphorylation at Thr-290 regulates Tpl2 binding to NF-kappaB1/p105 and Tpl2 activation and degradation by lipopolysaccharide. Proc Natl Acad Sci USA 102:2350–2355
15. Lang V, Symons A, Watton SJ, Janzen J, Soneji Y, Beinke S et al (2004) ABIN-2 forms a ternary complex with TPL-2 and NF-kappa B1 p105 and is essential for TPL-2 protein stability. Mol Cell Biol 24:5235–5248

16. Robinson MJ, Beinke S, Kouroumalis A, Tsichlis PN, Ley SC (2007) Phosphorylation of TPL-2 on serine 400 is essential for lipopolysaccharide activation of extracellular signal-regulated kinase in macrophages. Mol Cell Biol 27:7355–7364
17. Roget K, Ben-Addi A, Mambole-Dema A, Gantke T, Yang HT, Janzen J et al (2012) IkappaB kinase 2 regulates TPL-2 activation of extracellular signal-regulated kinases 1 and 2 by direct phosphorylation of TPL-2 serine 400. Mol Cell Biol 32:4684–4690
18. Rodriguez S, Abundis C, Boccalatte F, Mehrotra P, Chiang MY, Yui MA et al (2020) Therapeutic targeting of the E3 ubiquitin ligase SKP2 in T-ALL. Leukemia 34:1241–1252
19. Cai Z, Moten A, Peng D, Hsu CC, Pan BS, Manne R et al (2020) The Skp2 pathway: a critical target for cancer therapy. Semin Cancer Biol 67:16–33
20. Wang G, Wang J, Chang A, Cheng D, Huang S, Wu D et al (2020) Her2 promotes early dissemination of breast cancer by suppressing the p38 pathway through Skp2-mediated proteasomal degradation of Tpl2. Oncogene 39:7034–7050
21. Gkirtzimanaki K, Gkouskou KK, Oleksiewicz U, Nikolaidis G, Vyrla D, Liontos M et al (2013) TPL2 kinase is a suppressor of lung carcinogenesis. Proc Natl Acad Sci 110:E1470–E1479
22. Sun F, Qu Z, Xiao Y, Zhou J, Burns TF, Stabile LP et al (2016) NF-kappaB1 p105 suppresses lung tumorigenesis through the Tpl2 kinase but independently of its NF-kappaB function. Oncogene 35:2299–2310
23. Decicco-Skinner KL, Trovato EL, Simmons JK, Lepage PK, Wiest JS (2011) Loss of tumor progression locus 2 (tpl2) enhances tumorigenesis and inflammation in two-stage skin carcinogenesis. Oncogene 30:389–397
24. Koliaraki V, Roulis M, Kollias G (2012) Tpl2 regulates intestinal myofibroblast HGF release to suppress colitis-associated tumorigenesis. J Clin Investig 122:4231–4242
25. Serebrennikova OB, Tsatsanis C, Mao C, Gounaris E, Ren W, Siracusa LD et al (2012) Tpl2 ablation promotes intestinal inflammation and tumorigenesis in Apcmin mice by inhibiting IL-10 secretion and regulatory T-cell generation. Proc Natl Acad Sci 109:E1082–E1091
26. Serebrennikova OB, Paraskevopoulou MD, Aguado-Fraile E, Taraslia V, Ren W, Thapa G et al (2019) The combination of TPL2 knockdown and TNFalpha causes synthetic lethality via caspase-8 activation in human carcinoma cell lines. Proc Natl Acad Sci 116:14039–14048
27. Davies CC, Mak TW, Young LS, Eliopoulos AG (2005) TRAF6 is required for TRAF2-dependent CD40 signal transduction in nonhemopoietic cells. Mol Cell Biol 25:9806–9819
28. Moschonas A, Kouraki M, Knox PG, Thymiakou E, Kardassis D, Eliopoulos AG (2008) CD40 induces antigen transporter and immunoproteasome gene expression in carcinomas via the coordinated action of NF-kappaB and of NF-kappaB-mediated de novo synthesis of IRF-1. Mol Cell Biol 28:6208–6222
29. Eliopoulos AG, Stack M, Dawson CW, Kaye KM, Hodgkin L, Sihota S et al (1997) Epstein-Barr virus-encoded LMP1 and CD40 mediate IL-6 production in epithelial cells via an NF-kappaB pathway involving TNF receptor-associated factors. Oncogene 14:2899–2916
30. Pucci B, Indelicato M, Paradisi V, Reali V, Pellegrini L, Aventaggiato M et al (2009) ERK-1 MAP kinase prevents TNF-induced apoptosis through bad phosphorylation and inhibition of Bax translocation in HeLa Cells. J Cell Biochem 108:1166–1174
31. Davies CC, Bem D, Young LS, Eliopoulos AG (2005) NF-kappaB overrides the apoptotic program of TNF receptor 1 but not CD40 in carcinoma cells. Cell Signal 17:729–738
32. Grashoff C, Hoffman BD, Brenner MD, Zhou R, Parsons M, Yang MT et al (2010) Measuring mechanical tension across vinculin reveals regulation of focal adhesion dynamics. Nature 466:263–266
33. Michael KE, Dumbauld DW, Burns KL, Hanks SK, Garcia AJ (2009) Focal adhesion kinase modulates cell adhesion strengthening via integrin activation. Mol Biol Cell 20:2508–2519
34. Eliopoulos AG, Das S, Tsichlis PN (2006) The tyrosine kinase Syk regulates TPL2 activation signals. J Biol Chem 281:1371–1380
35. Cooper J, Giancotti FG (2019) Integrin signaling in cancer: mechanotransduction, stemness, epithelial plasticity, and therapeutic resistance. Cancer Cell 35:347–367
36. Funakoshi-Tago M, Sonoda Y, Tanaka S, Hashimoto K, Tago K, Tominaga S et al (2003) Tumor necrosis factor-induced nuclear factor kappaB activation is impaired in focal adhesion kinase-deficient fibroblasts. J Biol Chem 278:29359–29365
37. Huang H, Zhao W, Yang D (2012) Stat3 induces oncogenic Skp2 expression in human cervical carcinoma cells. Biochem Biophys Res Commun 418:186–190
38. Wei Z, Jiang X, Qiao H, Zhai B, Zhang L, Zhang Q et al (2013) STAT3 interacts with Skp2/p27/p21 pathway to regulate the motility and invasion of gastric cancer cells. Cell Signal 25:931–938
39. Wang ST, Ho HJ, Lin JT, Shieh JJ, Wu CY (2017) Simvastatin-induced cell cycle arrest through inhibition of STAT3/SKP2 axis and activation of AMPK to promote p27 and p21 accumulation in hepatocellular carcinoma cells. Cell Death Dis 8:e2626
40. Johnson DE, O'Keefe RA, Grandis JR (2018) Targeting the IL-6/JAK/STAT3 signalling axis in cancer. Nat Rev Clin Oncol 15:234–248
41. Waterfield MR, Zhang M, Norman LP, Sun SC (2003) NF-kappaB1/p105 regulates lipopolysaccharide-stimulated MAP kinase signaling by governing the stability and function of the Tpl2 kinase. Mol Cell 11:685–694
42. Kearney CJ, Sheridan C, Cullen SP, Tynan GA, Logue SE, Afonina IS et al (2013) Inhibitor of apoptosis proteins (IAPs) and their antagonists regulate spontaneous and tumor necrosis factor (TNF)-induced proinflammatory cytokine and chemokine production. J Biol Chem 288:4878–4890
43. Bertrand MJ, Milutinovic S, Dickson KM, Ho WC, Boudreault A, Durkin J et al (2008) cIAP1 and cIAP2 facilitate cancer cell survival by functioning as E3 ligases that promote RIP1 ubiquitination. Mol Cell 30:689–700
44. Festjens N, Vanden Berghe T, Cornelis S, Vandenabeele P (2007) RIP1, a kinase on the crossroads of a cell's decision to live or die. Cell Death Differ 14:400–410
45. Pickup MW, Mouw JK, Weaver VM (2014) The extracellular matrix modulates the hallmarks of cancer. EMBO Rep 15:1243–1253
46. Giancotti FG, Ruoslahti E (1999) Integrin signaling. Science 285:1028–1032
47. Schwartz MA, Assoian RK (2001) Integrins and cell proliferation: regulation of cyclin-dependent kinases via cytoplasmic signaling pathways. J Cell Sci 114:2553–2560
48. Gerard C, Goldbeter A (2014) The balance between cell cycle arrest and cell proliferation: control by the extracellular matrix and by contact inhibition. Interface focus 4:20130075
49. Jacque E, Schweighoffer E, Visekruna A, Papoutsopoulou S, Janzen J, Zillwood R et al (2014) IKK-induced NF-kappaB1 p105 proteolysis is critical for B cell antibody responses to T cell-dependent antigen. J Exp Med 211:2085–2101
50. Miller TL, McGee DW (2002) Epithelial cells respond to proteolytic and non-proteolytic detachment by enhancing interleukin-6 responses. Immunology 105:101–110
51. He X, Chen X, Li B, Ji J, Chen S (2017) FAK inhibitors induce cell multinucleation and dramatically increase pro-tumoral cytokine expression in RAW 264.7 macrophages. FEBS Lett 591:3861–3871
52. Jiang H, Liu X, Knolhoff BL, Hegde S, Lee KB, Jiang H et al (2020) Development of resistance to FAK inhibition in pancreatic cancer is linked to stromal depletion. Gut 69:122–132

53. Murphy JM, Rodriguez YAR, Jeong K, Ahn EE, Lim SS (2020) Targeting focal adhesion kinase in cancer cells and the tumor microenvironment. Exp Mol Med 52:877–886
54. Gabriel B, zur Hausen A, Stickeler E, Dietz C, Gitsch G, Fischer DC et al (2006) Weak expression of focal adhesion kinase (pp125FAK) in patients with cervical cancer is associated with poor disease outcome. Clin Cancer Res 12:2476–2483
55. Ohta R, Yamashita Y, Taketomi A, Kitagawa D, Kuroda Y, Itoh S et al (2006) Reduced expression of focal adhesion kinase in intrahepatic cholangiocarcinoma is associated with poor tumor differentiation. Oncology 71:417–422
56. Ayaki M, Komatsu K, Mukai M, Murata K, Kameyama M, Ishiguro S et al (2001) Reduced expression of focal adhesion kinase in liver metastases compared with matched primary human colorectal adenocarcinomas. Clin Cancer Res 7:3106–3112
57. Maung K, Easty DJ, Hill SP, Bennett DC (1999) Requirement for focal adhesion kinase in tumor cell adhesion. Oncogene 18:6824–6828
58. Basson MD, Sanders MA, Gomez R, Hatfield J, Vanderheide R, Thamilselvan V et al (2006) Focal adhesion kinase protein levels in gut epithelial motility. Am J Physiol Gastrointest Liver Physiol 291:G491–G499
59. Hatziapostolou M, Polytarchou C, Panutsopulos D, Covic L, Tsichlis PN (2008) Proteinase-activated receptor-1-triggered activation of tumor progression locus-2 promotes actin cytoskeleton reorganization and cell migration. Cancer Res 68:1851–1861
60. Takahashi R, Sonoda Y, Ichikawa D, Yoshida N, Eriko AY, Tadashi K (2007) Focal adhesion kinase determines the fate of death or survival of cells in response to TNFalpha in the presence of actinomycin D. Biochem Biophys Acta 1770:518–526
61. Tenev T, Bianchi K, Darding M, Broemer M, Langlais C, Wallberg F et al (2011) The Ripoptosome, a signaling platform that assembles in response to genotoxic stress and loss of IAPs. Mol Cell 43:432–448
62. Feoktistova M, Geserick P, Kellert B, Dimitrova DP, Langlais C, Hupe M et al (2011) cIAPs block Ripoptosome formation, a RIP1/caspase-8 containing intracellular cell death complex differentially regulated by cFLIP isoforms. Mol Cell 43:449–463
63. Wu SZ, Roden DL, Wang C, Holliday H, Harvey K, Cazet AS et al (2020) Stromal cell diversity associated with immune evasion in human triple-negative breast cancer. EMBO J 39:e104063
64. Pelka K, Hofree M, Chen JH, Sarkizova S, Pirl JD, Jorgji V et al (2021) Spatially organized multicellular immune hubs in human colorectal cancer. Cell 184:4734–52.e20